p- and sd-shell Λ-hypernuclei with shell model approach

A. Umeya(*)

Liberal Arts and Sciences, Nippon Institute of Technology, Miyashiro, Saitama 345-8501, Japan

Summary. — As a higher stage of hypernuclear studies, new experiments with high intensity and high resolution are being planned at the Japan Proton Accelerator Research Complex and the Jefferson Laboratory. We focus our attention on the interplay between the hyperon motion and the nuclear core states. Taking two typical examples of the p-shell hypernucleus ${}^{10}_{\Lambda}$Be and the sd-shell hypernucleus ${}^{27}_{\Lambda}$Mg, we discuss novel coupling features of the p^{Λ} orbital and the core deformation within the extended shell-model framework.

1. – Introduction

Hypernuclear structure studies have been progressing steadily through the K- and π-induced production reaction experiments, especially by the γ-ray coincidence measurements with the large volume Ge detector [1]. Moreover a series of recent $(e, e'K^+)$ reaction experiments from the Jefferson Laboratory (JLab) provide high-resolution data of the low-lying energy levels for p-shell hypernuclei [2, 3]. These data are quite helpful in better understanding of hyperon-nucleon interactions, though the data are still limited to about ten hypernuclear species.

As a higher stage of hypernuclear studies, new projects of high-intensity and high-resolution $(K^-, \pi^-\gamma)$ and $(\pi^+, K^+\gamma)$ reaction experiments are being scheduled at the Japan Proton Accelerator Research Complex (J-PARC) facility. New experiments are also planned at JLab. In order to meet these experimental projects, updated theoretical studies are needed for prediction and/or comparison with the coming quality data.

The recent ${}^{10}\mathrm{B}\,(e, e'K^+)\,{}^{10}_{\Lambda}$Be reaction experiment done at JLab [4] provides us with an interesting new aspect that is not seen in ordinary nuclear structures. This high resolution experiment has confirmed the four major peaks predicted by the distorted-wave impulse approximation (DWIA) calculations [5] based on the normal-parity nuclear core wave functions coupled with a Λ hyperon in s orbit. At the same time, the data also show an extra subpeak (bump) which seems difficult to be explained within the p-shell nuclear normal-parity configurations employed so far.

(*) E-mail: aumeya@nit.ac.jp

In this article, we focus our attention on the interplay between the hyperon motion and the nuclear core states in typical p- and sd-shell hypernuclei. The extended shell-model calculation [6] proved to be successful for the first time in explaining the extra subpeak observed in the ${}^{10}\mathrm{B}\,(e,e'K^+)\,{}^{10}_{\Lambda}\mathrm{Be}$ experiment [4]. It is attributed to the lowering of $p^{\Lambda}_{//}$ state (See Fig. 1 for this notation) due to the strong coupling with α-α like nuclear core deformation as already known in the case of ${}^{9}_{\Lambda}\mathrm{Be}$ [7, 8]. In the sd-shell region, we will show the results of new calculations for a hypernuclear structure of ${}^{27}_{\Lambda}\mathrm{Mg}$, which is expected to be well produced by the ${}^{27}\mathrm{Al}\,(e,e'K^+)$ and ${}^{27}\mathrm{Al}\,(\pi^-,K^0)$ reactions. It is noted that the even-even core nucleus ${}^{26}\mathrm{Mg}$ is shown to have rotational bands. Thus we see interesting interplay in the coupling of the p^{Λ} orbital and the core deformation.

2. – Multi-configuration shell-model framework

In the extended shell-model calculation [6], each hypernuclear state of $J^{\pm}$ is described by taking four types configurations, (A) $[J^-_{\mathrm{core}(i)}\otimes s^{\Lambda}]_{J^-}$, (B) $[J^-_{\mathrm{core}(i)}\otimes p^{\Lambda}]_{J^+}$, (C) $[J^+_{\mathrm{core}(i)}\otimes s^{\Lambda}]_{J^+}$, and (D) $[J^+_{\mathrm{core}(i)}\otimes p^{\Lambda}]_{J^-}$, where s^{Λ} and p^{Λ} denote the Λ single-particle states. $J^{\pm}_{\mathrm{core}(i)}$ denotes all the possible spin-parity states of core nucleus, which are labeled with i. In the traditional treatments appeared so far, only (A) and (B) configurations are taken into account. However, we found it important to extend the model space to include (C) and (D) configurations as well. For the case of ${}^{10}_{\Lambda}\mathrm{Be}$, the natural-parity (unnatural-parity) core state $J^-_{\mathrm{core}(i)}$ ($J^+_{\mathrm{core}(i)}$) is constructed in the $0\hbar\omega$ ($1\hbar\omega$) space, and nuclear core configurations with natural- and unnatural-parity, (B) and (C), can be mixed easily by the ΛN interaction at appropriate excitation energy where the lowering of $p^{\Lambda}_{//}$ favors as mentioned above.

Secondly, in order to study coupling features of Λ and typical rotational motion, we further apply the extended shell model to sd-shell hypernuclei. For the core nucleus ${}^{26}\mathrm{Mg}$, natural-parity nuclear core states are described in the conventional model space as $|(0s)^4(0p)^{12}(sd)^{10};J^+_{\mathrm{core}(i)}\rangle$, and unnatural-parity nuclear core states are described by the $1p$-$1h$ $1\hbar\omega$ excitations as $|(0s)^4(0p)^{11}(sd)^{11};J^-_{\mathrm{core}(i)}\rangle$. For the single-particle states of the Λ hyperon, $0s$-, $0p$-, and sd-shell orbitals are taken into account, so that new configurations such as $[{}^{26}\mathrm{Mg}(J^{\pm}_{\mathrm{core}})\otimes(sd)^{\Lambda}]$ should be added. Thus each hypernuclear state of $J^{\pm}$ is described by taking six types configurations. For sd-shell hypernucleus ${}^{27}_{\Lambda}\mathrm{Mg}$, we will show interesting results from the first but limited calculation done within each of the configuration-diagonal spaces for the positive-parity core states.

3. – Results and discussion

In the ${}^{9}_{\Lambda}\mathrm{Be}$ hypernucleus, it is well known that the p^{Λ} state splits into two orbital states expressed by $p^{\Lambda}_{\perp}$ and $p^{\Lambda}_{//}$ as shown in Fig. 1. The splitting is due to the strong coupling with nuclear core deformation having the α-α structure [7, 8]. For the ${}^{9}\mathrm{Be}\,(K^-,\pi^-)$ reaction, the DWIA cross sections obtained by using the extended shell-model wave functions are in good agreement with those by using the cluster-model wave functions [7]. For the other p-shell hypernuclei, ${}^{10}_{\Lambda}\mathrm{Be}$, ${}^{10}_{\Lambda}\mathrm{B}$, and ${}^{11}_{\Lambda}\mathrm{B}$, the extended shell-model calculation also shows the p^{Λ}-state splitting [6, 9]. Especially, in the ${}^{10}_{\Lambda}\mathrm{Be}$ hypernucleus, the low-energy $p^{\Lambda}_{//}$ states can mix with s^{Λ} states. These parity-mixed wave functions can explain, for the first time, the extra subpeak observed in the ${}^{10}\mathrm{B}\,(e,e'K^+)\,{}^{10}_{\Lambda}\mathrm{Be}$ reaction experiment.

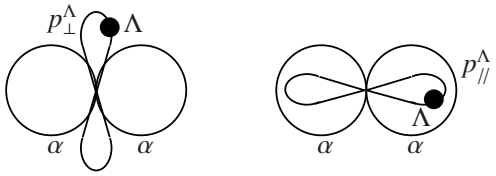

Fig. 1. – The $p^{\Lambda}_{\perp}$ (left) and $p^{\Lambda}_{//}$ (right) states realized in ${}^{9}_{\Lambda}$Be due to the α-α core deformation.

Figure 2 shows the calculated energy levels of ${}^{27}_{\Lambda}$Mg, together with the low-lying energy levels of ^{26}Mg. For ^{26}Mg, the calculated energy levels are in good agreement with the experimental levels. For ${}^{27}_{\Lambda}$Mg, the low-lying hypernuclear states consist of the $0s^{\Lambda}$ single-particle state. We note that the energy spacings of the $5/2^{+}_{1}$-$3/2^{+}_{1}$ ($5/2^{+}_{2}$-$3/2^{+}_{2}$) doublet with the 2^{+}_{1} (2^{+}_{2}) core state is narrow. This is attributed to the small spin-orbit component of the ΛN interaction adopted reasonably in this calculations. One notes also that the contribution from ΛN spin-spin component is small.

The Anti-symmetrized Molecular Dynamics (AMD) calculation provides the detailed analyses of the rotational bands in the ^{26}Mg nucleus [10]. In the present shell-model calculation, we obtain four rotational bands with the help of $B(E2)$ estimates for possible transitions. One notices that in the ${}^{9}_{\Lambda}$Be case the nuclear core deformation is based on the dumbbell structure of the α-α system, while in ^{26}Mg the rotational motion is mainly based on the quadrupole deformation. Here we remark that the large scale shell model within certain limitation works in describing effectively the various kinds of rotational states as far as the amount of deformation is tractable. Figure 3 shows these bands in the energy levels of ^{26}Mg, together with strengths of $E2$ transitions. The first column shows the ground band. In the theoretical $B(E2)$ estimates, the effective charges are adjusted to reproduce the experimental $B(E2; 2^{+}_{1} \rightarrow 0^{+}_{\text{g.s.}})$ value of $61.3\, e^2\text{fm}^4$. The numerical results help us to classify the calculated energy levels into the members belonging to four rotational bands, respectively, since intra-band $B(E2)$ cascades are obtained in the present shell-model calculation. The 2^{+}_{1} state is in the ground band, and the 2^{+}_{2} state

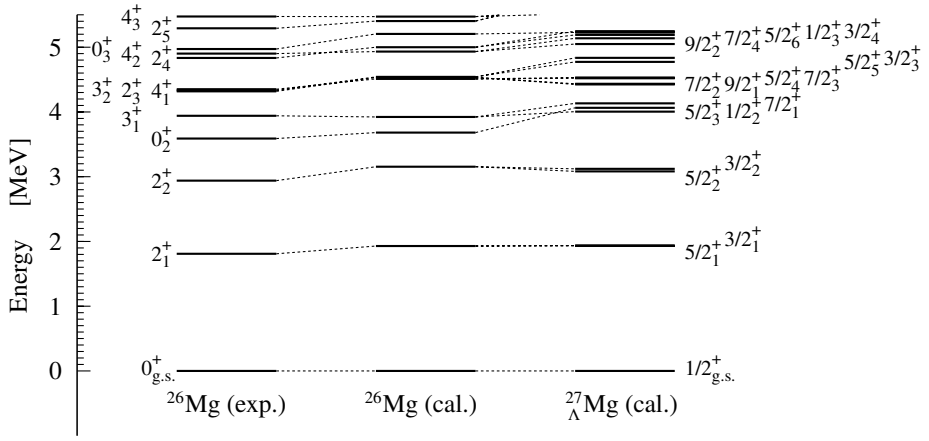

Fig. 2. – Calculated energy levels of ${}^{27}_{\Lambda}$Mg (right column), together with the experimental and calculated levels of ^{26}Mg (central and left columns).

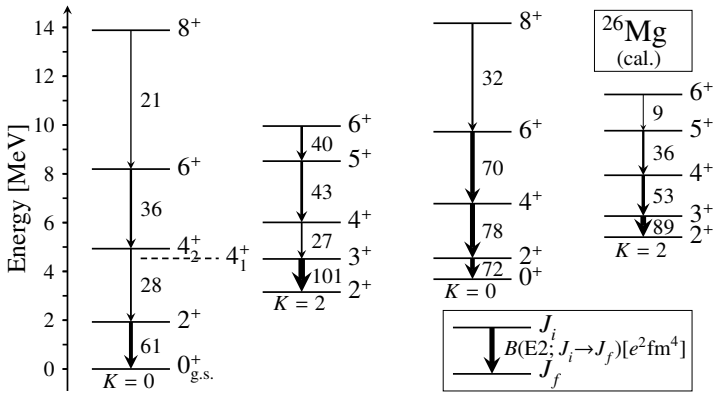

Fig. 3. – Rotational bands in the energy levels of ^{26}Mg, together with strengths of $E2$ transitions. The arrows denote $E2$ transitions.

is the band head of the rotational band with $K = 2$. The property of these rotational level structures has been pointed out in the AMD calculation [10].

In hypernuclei, a Λ hyperon in the p^Λ orbits induces a mixing of nuclear core states by ΛN interaction, while that in the s^Λ orbit does not. In the low-lying negative-parity states of heavier hypernuclei $^{145-155}_{\Lambda}$Sm, a covariant density functional theory suggested that the admixture of the p^Λ configurations coupled with nuclear core states having J_{core} and $J_{\mathrm{core}} \pm 2$ [11]. This mechanism generally applies to the Λ-particle-rotor coupling systems. In fact we found that the similar mixing occurs in the *sd*-shell hypernucleus $^{27}_{\Lambda}$Mg. For example, in the present shell-model calculation, configurations of the $^{27}_{\Lambda}$Mg negative-parity states $1/2^-$ ($E_x^{\mathrm{cal}} = 10.615\,\mathrm{MeV}$) and $3/2^-$ ($E_x^{\mathrm{cal}} = 10.685\,\mathrm{MeV}$) are

$$(1) \quad |1/2^-\rangle = \sqrt{0.70}\,|0^+_{\mathrm{g.s.}} \otimes p^\Lambda_{1/2}\rangle + \sqrt{0.28}\,|2^+_1 \otimes p^\Lambda_{3/2}\rangle + \cdots,$$

$$(2) \quad |3/2^-\rangle = \sqrt{0.68}\,|0^+_{\mathrm{g.s.}} \otimes p^\Lambda_{3/2}\rangle + \sqrt{0.15}\,|2^+_1 \otimes p^\Lambda_{3/2}\rangle - \sqrt{0.15}\,|2^+_1 \otimes p^\Lambda_{1/2}\rangle + \cdots,$$

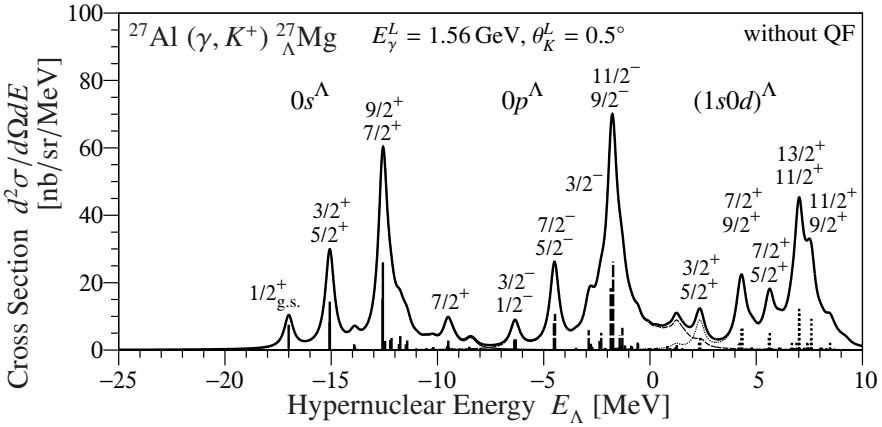

Fig. 4. – The DWIA cross sections of the ^{27}Al (γ, K^+) $^{27}_{\Lambda}$Mg reaction without quasi-free (QF) contribution. The solid, dashed, and dotted bars denote s^Λ, p^Λ, and $(sd)^\Lambda$ states, respectively.

respectively. The mixing amplitudes are quite large in these negative-parity states which consist of the p-state Λ particle and the deformed core. On the other hand, configurations of the ${}^{27}_{\Lambda}$Mg positive-parity states $1/2^+_{\rm g.s.}$, $5/2^+_1$ ($E_x^{\rm cal} = 1.932\,{\rm MeV}$), and $3/2^+_1$ ($E_x^{\rm cal} = 1.935\,{\rm MeV}$) are $|1/2^+\rangle = \sqrt{0.99}\,|0^+_{\rm g.s.} \otimes s^{\Lambda}_{1/2}\rangle + \cdots$, $|5/2^+\rangle = \sqrt{0.99}\,|2^+_1 \otimes s^{\Lambda}_{1/2}\rangle + \cdots$, and $|3/2^+\rangle = \sqrt{0.99}\,|2^+_1 \otimes s^{\Lambda}_{1/2}\rangle + \cdots$, respectively. Due to the weak coupling between the nuclear core and the Λ hyperon in the s orbit which is completely spherical, the $s^{\Lambda}_{1/2}$ hyperon does not induce a mixing of nuclear core states.

Figure 4 shows the DWIA calculation of the ${}^{27}{\rm Al}\,(\gamma, K^+)\ {}^{27}_{\Lambda}$Mg reaction cross sections. The ${}^{27}_{\Lambda}$Mg hypernucleus can be obtained by the ${}^{27}{\rm Al}\,(e, e'K^+)$ reaction experiment at JLab and the ${}^{27}{\rm Al}\,(\pi^-, K^0)$ reaction experiment at J-PARC. In the future work, comparing the DWIA cross sections of these hypernuclear productions within the extended shell-model framework is valuable to understand the structure of the ${}^{27}_{\Lambda}$Mg hypernucleus.

4. – Concluding remarks

We have investigated the structures of the ${}^{10}_{\Lambda}$Be and ${}^{27}_{\Lambda}$Mg hypernuclei by using the extended shell-model framework. Strong coupling between p^{Λ} state and core deformation is realized in these hypernuclei. In ${}^{10}_{\Lambda}$Be, the p^{Λ} state splits into $p^{\Lambda}_{\perp}$ and $p^{\Lambda}_{/\!/}$ states under the strong effect of the nuclear core deformation, and the lower $p^{\Lambda}_{/\!/}$ state comes down in energy and couples easily with s^{Λ} state coupled with different parity core-excited states. In ${}^{27}_{\Lambda}$Mg, the low-lying negative-parity states show large admixture of the p^{Λ} configurations coupled with nuclear core states having 0^+ and 2^+, which manifests one of the general properties for the Λ particle plus nuclear rotor systems. It should be remarked that the present large scale shell model is effective also in describing certain amount of deformed hypernuclear systems. The wave functions are used to predict the (γ, K^+) spectrum for future experiments.

* * *

The author thanks Dr. T. Motoba and Dr. K. Itonaga for collaboration and discussions. This work was supported by JSPS KAKENHI Grant Number JP20K03950.

REFERENCES

[1] Hashimoto O. and Tamura H., *Prog. Part. Nucl. Phys.*, **57** (2006) 564, and references therein.
[2] Gogami T. *et al.*, *Phys. Rev. C*, **103** (2021) L041301, and references therein.
[3] Urciuoli G. M. *et al.*, *Phys. Rev. C*, **91** (2015) 034308, and references therein.
[4] Gogami T. *et al.*, *Phys. Rev. C*, **93** (2016) 034314.
[5] Motoba T., Sotona M. and Itonaga K., *Prog. Theor. Phys. Suppl.*, **117** (1994) 123.
[6] Umeya A., Motoba T. and Itonaga K., *JPS Conf. Proc.*, **26** (2019) 023016; *J. Phys. Conf. Ser.*, **1643** (2020) 012110.
[7] Bandō H., Seki M. and Shono Y., *Prog. Theor. Phys.*, **66** (1981) 2118; Motoba T., Bandō H. and Ikeda K., *Prog. Theor. Phys.*, **70** (1983) 189.
[8] Dalitz R. H. and Gal A., *Phys. Rev. Lett.*, **36** (1976) 362; *Ann. Phys.*, **131** (1981) 314.
[9] Umeya A., Motoba T. and Itonaga K., *Proc. of Sci.*, **380** (2022) 213; *EPJ Web of Conf.*, **271** (2022) 01010.
[10] Kanada-En'yo Y., Shikata Y., Chiba Y. and Ogata K., *Phys. Rev. C*, **102** (2020) 014607.
[11] Mei H., Hagino K., Yao J. M. and Motoba T., *Phys. Rev. C*, **96** (2017) 014308.